Spatio-temporal Analysis of an HLB Epidemic in Florida and Implications for Spread

T. R. Gottwald[1], M. S. Irey[2], T. Gast[2], S. R. Parnell[3], E. L. Taylor[1] and M. E. Hilf[1]

[1]USDA, ARS, US Horticultural Research Laboratory, Fort Pierce, FL, 34945
[2]Southern Gardens, US Sugar Corp., Clewiston, FL, 33440
[3]Biomathematics and Bioinformatics, Rothamsted Research, Harpenden, AL5 2JQ, UK

ABSTRACT: Data for Huanglongbing (HLB) epidemics were collected during five assessment dates over a 2-yr period from 11, 4-ha commercial citrus blocks in Florida. Data were analyzed for regional spatial characteristics via Ripley's K analyses. Data were fitted to the logistic and Gompertz temporal models, the latter proving to be the superior to represent the increase of HLB through time. Data were also examined using the spatio-temporal stochastic model for disease spread which was fitted using (MCMC) stochastic integration methods. The Ripley's *K* analyses demonstrated a continuous relationship among HLB-diseased individuals over a broad range of spatial distances up to 3.5 km, demonstrating short range to regional components for HLB spread by psyllid vectors with a most common distance of 1.58 km which may indicate an average psyllid dispersal distance from a regional point of view. The results of the spatio-temporal analysis were viewed graphically in a two-dimensional parameter space representing a series of 'posterior density' contours of parameter densities. The spatio-temporal model suggested that HLB spread through a combination of random 'background' transmission and a 'local' transmission that operated over short distances. However, background versus local transmission often did not always occur simultaneously but often alternated. If we consider that the background transmission or primary infection is the result of inoculum sources outside the plots, then this is similar to the spatio-temporal stochastic model results for *Citrus tristeza virus* and other pathosystems with vectors predominately of the migratory type. That is, infective psyllids periodically emigrated from outside the plots and infected test trees causing background or primary infection and then infective psyllids from within the plots caused local or secondary spread.

Relatively few quantitative epidemiological studies have been conducted on the epidemiology of huanglongbing (HLB). This is true for many fastidious arboreal plant pathosystems like HLB. This is due to the perennial nature of the disease and host and, until the recent development and use of polymerase chain reaction (PCR) for detection of the putative pathogen, was based on monitoring on visual assessment of disease symptoms over multiple years. In addition, it has been difficult to locate study sites where the disease is allowed to progress unimpeded so epidemics can be followed without intervention of control activities. This is due to the devastating results of HLB infection and the fear of allowing uncontrolled inoculum sources to exist in a region with susceptible plantings (2, 3, 17).

Monitoring the occurrence of symptoms can be somewhat problematic for HLB. Typical leaf mottling and chlorosis similar to zinc deficiency pattern are usually followed by retarded growth, but these symptoms are often indistinct and/or restricted to one branch or side of the tree and can be easily overlooked when assaying entire plantings (10, 22, 25). The lag in time between transmission of the pathogen by psyllid vectors (*Diaphorina citri*) or by propagation and the onset of visual symptoms can be quite variable depending on the time of the year when infection took place, ensuing environmental conditions, tree age, species/cultivar and horticultural health, etc. (1, 6, 16, 23). Thus, visually

quantifying the severity or expression of disease symptoms in individual trees is not a true indication of pathogen content. Additionally, due to the temporal variation in symptom expression, trees infected at the same time (especially trees of several years age) may express the onset of infection with great variability over one or more years. This inherently broad and variable lag period, compromises the accuracy of spatial and temporal studies to some extent. Because visual symptoms seen at any point in time are the expression of infections that have occurred and/or accumulated sometime in the past, thus, these observations are actually an assessment of a 'fuzzy history' of infection as it exists at a time period in the past equivalent to the lag period. Nevertheless, with these caveats in mind, useful information can still be gleaned from the epidemiological studies conducted to date concerning the spatial processes that give rise to HLB disease progress. An understanding of this information can be used to predict the economic life of a given planting and a means to investigate efficacy of possible control interventions.

The spatial and temporal dynamics of HLB in mature plantings has been investigated in only very few cases, primarily from Reunion Island and China (15, 16, 17, 19). More recently, studies are being conducted in Brazil and Florida. In all prior cases, only the Asian HLB pathogen, "*Candidatus* Liberibacter asiaticus", was known to be present. With the discovery of "*Ca.* L. americanus" in São Paulo, Brazil, some data on disease increase and spread of that organism is being collected as well (4). Prior studies presented an opportunity to investigate the disease in citrus plantings in two situations, where inoculum was introduced by infected planting stock, and where clean stock was utilized and the pathogen was introduced by the migration of bacteria-contaminated psyllid vectors. The studies were conducted to establish preliminary rates of disease increase of citrus HLB under endemic conditions in the presence of vector populations, and develop preliminary temporal models to estimate the expected longevity of infected sweet orange and mandarin plantings.

Previous studies of HLB increase and spread conducted in China and Reunion Island, indicate a rate of disease increase leading to a multi-year epidemic similar to the *Citrus tristeza virus-Aphis gossypii* pathosystem. In contrast, more recent studies in Brazil and Vietnam suggest a much more rapid rate of disease increase and spread (4, 6, 9, 17).

In the present study, HLB incidence was examined in a previously uninfected large >4,800 ha plantation in South Florida where no new citrus had been introduced for 10 yr and thus infection was entirely dependent on psyllid transmission. Objectives of this study were: 1) to characterize relationships of HLB-positive trees across a range of distances from immediately adjacent trees to regionally to gain insights into psyllid transmission, and 2) to use stochastic modeling methods to parse disease spread over time into components using likelihood estimates of the 'primary infection rate' (introduction from outside the area under study) and 'secondary infection' (spread locally within the area of study).

MATERIALS AND METHODS

Data collection. Based on the commercial survey of trees with visual symptoms of HLB, the spatial pattern of HLB was determined over a large contiguous planting of citrus 4,856 ha in South Florida. The area was completely surveyed via a 100% census of trees five times (Z_1-Z_5) over a 2-yr period. The commercial planting was a mixture of sweet orange cultivars, predominately Valencia and Hamlin on various rootstocks. A subsection of the plantation composed of 180 blocks (~739 ha) was used for the study. Block size varied little across the subsection of the planting with a standard block composed of 14 rows of 110-115 plants/row and thus ~1,500 trees/block. Incidence of HLB was assessed by visual inspection of the canopies of all trees in each plot by professional scouts. Because of the size of the total plantation, assays of each block were not always contemporaneous and therefore, the assay date relative to individual blocks was utilized. The GIS location of each symptomatic tree and the date when the symptoms were assessed were recorded on GIS referenced maps of the plantation. Incidence of individual blocks varied from 0 to 0.44 over the duration of the study.

Regional Spatial Analysis. Because of the unprecedented size of the data set, the data presented a unique opportunity to examine HLB spatial relationships at the 'regional' spatial scale for the first time. This allowed us to determine the relationships among HLB-diseased plants over a range of immediately adjacent to very large distances. Binary spatial maps of HLB were prepared for all assessment dates for the entire section of the plantation. To assess the spatial distribution on a regional level, this entire map consisting of >250,000 trees distributed over 729 ha was examined via a modified Ripley's *K*-function spatial point pattern analysis method for each of the five assessments (8, 21). Evaluation of the spatial point pattern (SPP) of HLB from a regional perspective was determined by an examination of differences between the spatial distribution of HLB-infected trees versus citrus trees in general within the study area. This was accomplished by comparing two cumulative distribution functions (cdf's): one representing the fraction of infected tree pairs less than or exactly a distance *d* apart [cdf I(*d*)] and the second distribution for the total population of trees [cdf T(*d*)]. Assuming that out of a total of N trees in the study site, *I* are HLB-infected. These cdf's can be expressed as:

$$cdf_T(d) = \frac{2\sum_{j=1}^{N}\sum_{k>j}^{N} m_{jk}}{N\cdot(N-1)} \quad (1)$$

$$cdf_I(d) = \frac{2\sum_{j=1}^{I}\sum_{k>j}^{I} s_{jk}}{I\cdot(I-1)} \quad (2)$$

where m=1 for tree pairs that are $\leq d_i$ apart and m=0 otherwise and likewise s=1 for infected tree pairs that are $\leq d_i$ apart and s=0 otherwise. The complete spatial randomness (CSR) assumption translates to the expected equivalence of Eqs. 1 and 2, so that a constant fraction $\{ I(I\text{-}1) / [N(N\text{-}1)]\}$ of tree pairs are infected, irrespective of distance *d*. The factor of '2' in the numerators of Eqs. 1 and 2 accounts for the fact that the pairs are unordered (i.e., $k>j$ in second summations for Eqs. 1 and 2). For a particular distance, *d*, the probability of selecting infected pairs in a sample of $N(N\text{-}1)/2 \cdot cdf_T(d)$ tree pairs chosen randomly from a population of size $N(N\text{-}1)/2$ of which $I(I\text{-}1)/2$ are infected is given by the hypergeometric distribution:

$$H\left(i,\frac{N(N-1)\cdot cdf_T(d)}{2},\frac{I(I-1)}{2},\frac{N(N-1)}{2}\right) \quad (3)$$

with mean value

$$i_{\exp}=\frac{I(I-1)\cdot cdf_T(d)}{2} \quad (4)$$

and variance

$$\sigma^2_{\exp}=i^2_{\exp}\cdot\left(1-cdf_T(d)\right)\cdot\left(1-\frac{I(I-1)}{N(N-1)}\right) \quad (5)$$

For the range of incidence and sample size examined in this study, the Hypergeometric function is well approximated by a Normal distribution with the same mean and variance. This fact can be used to estimate confidence intervals.

The HLB-infected trees are tested for spatial dependency by applying the one-sample sided single-tailed Kolmogorov-Smirnov test to the maximum distance {D = max [$cdf_I(d)$ - $cdf_T(d)$]} between the above two cumulative distributions (7). The above describes an analytical approach to SPP analysis that is an outgrowth of the modification to Ripley's *K*-function presented by Ward and Ferrandino (24). Note this analysis is equivalent to Ripley's *K*-function in the limit of an infinite number of trees uniformly covering the study site.

The above analysis was accomplished through the use of a Visual Basic program and compares the infected SPP to the total SPP. This generalized Ripley's *K*-function was used to examine SPP of the subsection of the plantation for each of the five assessments. Via this method, analytical results were obtained for the range of spatial dependency (RSD), i.e., the distance at which the estimated and observed cdf's in Eq. 1 intersect; the effective range of spatial dependency (RSD_{eff}), i.e. the distance over which the cdf's in Eq. 1 were significantly ($P<0.05$) different; the distance at which maximal spatial difference (MSD) occurred, and the cdf (*K*-value) associated with the maximum spatial difference (Max_{diff}).

Temporal and Spatio-temporal analysis. For temporal analyses of each of 11 selected citrus blocks, the disease incidence data over time (x) in days and years were first transformed via logistic and Gompertz linear transformations, logit(y) = ln(y/1-y) and Gompit(y) = -ln(-ln(y)), respectively, where y = disease incidence. The transformed data were then fitted via linear regression analysis. The appropriateness of the models were assessed by a combination of superior r^2 combined with examination of residuals of regression for trends and the proportion of both appropriate and superior fits of one model compared to the other.

For spatio-temporal analyses, data for each of the 11 HLB–infected blocks selected were also analyzed using the spatio-temporal stochastic model for disease spread which was fitted using Markov-Chain Monte Carlo (MCMC) stochastic integration methods. For a thorough description of the MCMC model, refer to Gibson (11, 12, 13, 18). The results of the spatio-temporal analysis can be viewed graphically in a two-dimensional parameter space representing a series of 'posterior density' contours of parameter densities, *L(a)*. The two parameters represent local (a_2) versus background (b) interactions. The parameter b quantifies the rate at which a susceptible individual acquires the disease due to 'primary infection' independent of the infected trees in the plot and therefore represents the simple interest or 'primary infection rate' in a spatio-temporal context. For many pathogens that are vector transmitted, this usually means from pathogen acquisition sources outside of the

host population, i.e., outside the plot. Whereas a_2 represents the 'secondary infection rate' in a spatio-temporal context, and quantifies the spread of the pathogen from an infected to a susceptible host plant by infected psyllids and the subsequent decrease in distance between infected trees. As a_2 increases, the secondary transmissions occur over shorter ranges and so as long as *b* is not so large that primary infections dominate, disease maps generated by the model exhibit aggregation. The MCMC analysis is accomplished by a simulation model that requires intensive computer memory because of the large number of comparisons it makes between individual plants in a matrix drawn from each of a substantial number of simulations (usually 500-1,000). All of these are held in memory and represent numerous, continuously updating calculations. The citrus blocks studied were too large to always allow this program to run due to memory restrictions. Thus, each plot was subdivided into two smaller plots each with <750 trees.

RESULTS AND DISCUSSION

Temporal progress of HLB. Temporal analyses indicated that the Gompertz model best represented the change in disease incidence over time for 10/11 = 90.1% of the plots. This is not surprising as the Gompertz model is considered the more versatile of the two models tested. The r^2 of the Gompertz model ranged from 0.61 to 0.94 and averaged 0.819 across the 11 plots (Fig. 1 and Table 1). The slopes of the regression lines are represented by Gompertz (*k*) values and equal to apparent infection rates of disease increase of HLB calculated on both a daily and yearly basis for comparison with other prior data. Daily, k_{da}, and yearly, k_{yr}, Gompertz rates of disease increase ranged from 0.0012 to 0.0027 and 0.4353 to 0.9720, respectively. The range of apparent infection rates from the 11 south Florida blocks circumscribed the rates obtained in the 1970s from Reunion Island and China but in some cases were even more rapid and consistent with recent observations from Brazil, Vietnam, etc. (4, 9, 14). Thus, in south Florida, at least for this one large study area, rates of HLB increase were similar to, and in some cases, more rapid that those in the literature.

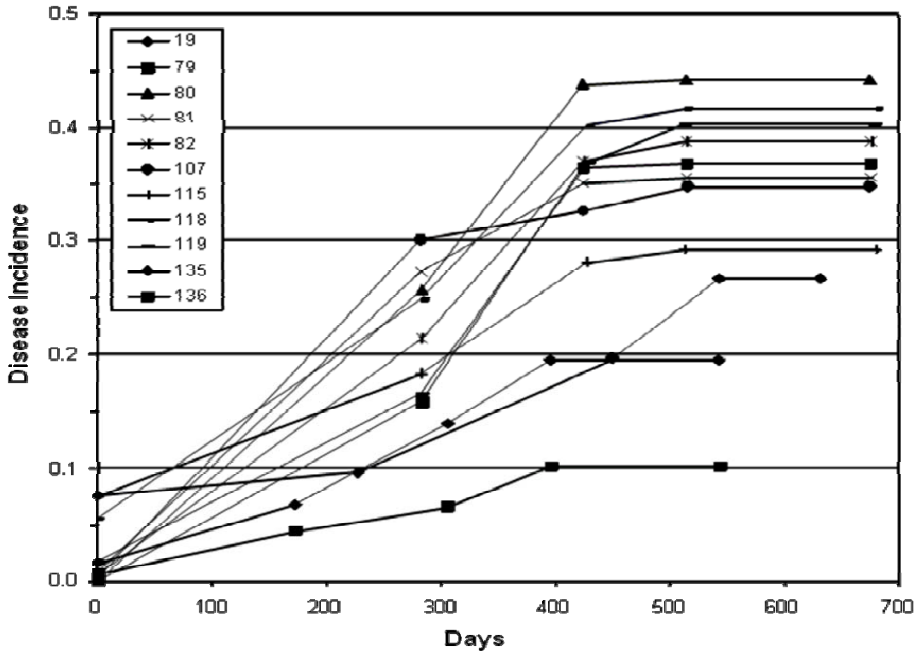

Fig. 1. Disease progress of citrus huanglongbing in 11 commercial citrus plantings in south Florida. Logistic and Gompertz models were fitted to each progress curve – modeling results are presented in Table 1.

TABLE 1
TEMPORAL ANALYSES OF HLB DISEASE INCREASE IN COMMERCIAL CITRUS PLANTINGS IN SOUTH FLORIDA

Logistic Model

Plot	R^2	Adj R^2	Std Error of (R^2)	$\boldsymbol{b}_{da}$ (Days)	Std Error of $\boldsymbol{b}_{da}$	$\boldsymbol{b}_{yr}$ (Years)	Std Error of $\boldsymbol{b}_{yr}$
19	0.9507	0.9343	0.1790	0.0027	0.0004	0.9787	0.5550
79	0.6086	0.4129	0.4319	0.0027	0.0015	0.9787	0.5550
80	0.6133	0.4199	0.3162	0.0020	0.0011	0.7236	0.4063
81	0.7508	0.6677	1.0737	0.0063	0.0021	2.3074	0.7675
82	0.8029	0.7371	1.0621	0.0073	0.0021	2.6537	0.7592
107	0.7218	0.6291	1.3681	0.0075	0.0027	2.7326	0.9795
115	0.8799	0.8398	0.2819	0.0026	0.0005	0.9404	0.2006
118	0.8606	0.8141	0.4644	0.0039	0.0009	1.4220	0.3305
119	0.8724	0.8298	0.6564	0.0058	0.0013	2.1147	0.4670
135	0.8777	0.8369	0.4712	0.0053	0.0011	1.9179	0.4134
136	0.8294	0.7725	0.5633	0.0052	0.0014	1.8845	0.4935

Gompertz Model

Plot	R^2	Adj R^2	Std Error of (R^2)	k_{da} (Days)	Std Error of K_{da}	k_{yr} (Years)	Std Error of k_{yr}

19	0.9402	0.9203	0.0891	0.0012	0.0002	0.4369	0.0636
79	0.6101	0.4151	0.2331	0.0015	0.0008	0.5297	0.2995
80	0.6148	0.4222	0.1937	0.0012	0.0007	0.4447	0.2489
81	0.7854	0.7139	0.3591	0.0023	0.0007	0.8505	0.2567
82	0.8546	0.8061	0.3239	0.0027	0.0006	0.9720	0.2315
107	0.7476	0.6635	0.4274	0.0025	0.0008	0.9123	0.3060
115	0.8912	0.8550	0.1234	0.0012	0.0002	0.4353	0.0878
118	0.8836	0.8447	0.2038	0.0019	0.0004	0.6920	0.1450
119	0.9011	0.8682	0.2375	0.0024	0.0005	0.8837	0.1690
135	0.9119	0.8825	0.1373	0.0018	0.0003	0.6714	0.1205
136	0.8771	0.8361	0.1318	0.0015	0.0003	0.5344	0.1155

Model parameters were estimated by linear regression of disease incidence of HLB+ trees transformed by $\ln(y/1-y)$ and $-\ln(-\ln(y))$, where y = disease incidence and b and k are the rate parameters for the logistic and Gompertz models, respectively versus time in either days or years. The rates were calculated on the basis of both day ($-b_{da}$ and k_{da}), and year ($-b_{yr}$ and k_{yr}), respectively, to allow comparison with other published rates of HLB increase.

Indications of regional spread. The results of the modified Ripley's *K*-function spatial point pattern analysis for each of the SPP for each of the five assessment dates gave strong indications of regional spread of HLB (Fig. 2). Aggregation of the SPP shown by a significant difference between cumulative distribution functions in Eqs. 1 and 2 above, was exhibited for all five of the respective assessments. The range of spatial dependency (RSD) was equal to the RSD_{eff} for all of the five assessment dates and thus indicated a departure from CSR over the majority to the entire range of 350 distance increments tested from 0 to 4.6 km. The range of spatial dependency was 3.32 to 3.5 km with a median distance of 3.5 km and was relatively stable through time. This indicated a departure from CSR throughout the epidemic period studied and a spatial structure of HLB-infected trees that were highly spatially related over large distances. This regional relationship among HLB-infected trees was investigated further by examining the calculated distance at which maximal spatial difference (MSD) occurred. The cdf (*K*-value) associated with the maximum spatial difference (Max_{diff}) is shown for all five assessments as well (Fig. 2 – vertical dotted line). The Max_{diff} ranged from 0.88 to 1.61 km with a median of 1.58 km and appeared to increase over time with disease incidence over the 2-yr period of the test. The Max_{diff} is an estimate of the most common distance between pairs of HLB-infected trees and thus allows some interpretation of the underlying spatial processes that may be involved on a regional scale. Thus, Max_{diff} suggests that there is a spatial relationship that is repeated most frequently at about 1.58 km, and may well indicate a common or average distance for psyllid dispersal of HLB regionally.

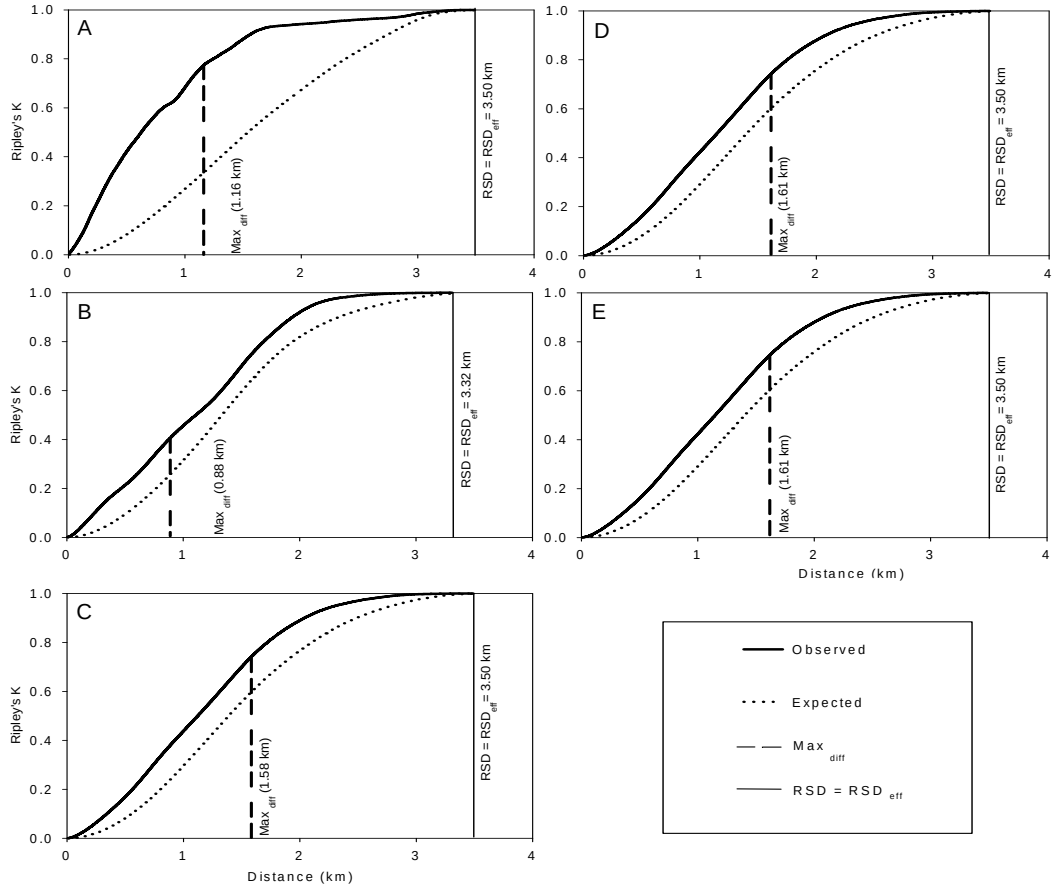

Fig. 2. Modified Ripleys *K* function analysis for the huanglongbing spatial point pattern for five assessments/surveys (A-E) of a large commercial citrus plantation in south Florida. Expected and observed cumulative distribution functions (cdf) are represented by the dotted and bold solid lines, respectively. RSD and RSD_{eff} are the range of spatial dependency and effective range of spatial dependency expressed in km (thin solid line). Max_{diff} = the maximum departure from randomness (maximum difference between expected and observed cdf) is expressed as distance in km (dashed line).

Spatio-temporal stochastic model MCMC. The second objective of the study was to parse the spatial spread of HLB into distinct and identifiable components. This was done by the use of MCMC stochastic modeling methods to give likelihood estimates of the 'primary infection rate' (introduction from outside the area under study) and 'secondary infection' (spread locally within the area of study). This was done via a stochastic model used previously and found to be useful to examine the spatio-temporal dynamics of the citrus tristeza, blight, psorosis and other pathosystems and the involvement and dynamics associated with various vector populations (5, 18, 20). Figs. 3-5 show the contour plots from 11 blocks subdivided into two smaller plots each for a total of 22 plots. Such subdivision of plots into smaller areas was necessary to accommodate the calculations as described above. For each of the 22 plots, spatial disease spread between two assessment times was analyzed via the MCMC model when a minimum increase in disease incidence of 2.5% had occurred. Examples of posterior density contour graphs are shown in Figs. 3-5 for which the MCMC program converged to a solution. These graphs are arranged into three groups

which share common characteristics among their posterior density contour graphs. Not all posterior density contour graphs are shown, as there are more than can be presented easily in multi-panel figures. Rather, representative contour graphs illustrating the range and prevalence of stochastic model results are shown.

The overall interpretation of the MCMC model analyses, considering all data sets, is that there were two spatial processes that were ongoing during HLB epidemics, but not necessarily simultaneously. First, note the posterior density contour graphs shown in Fig. 3.

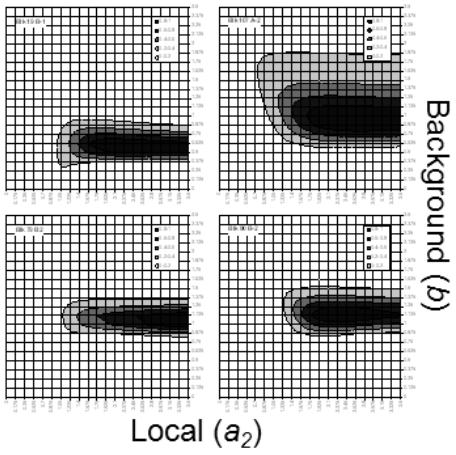

Fig. 3. Posterior density estimates of Markov-Chain Monte Carlo Simulation of the Spatio-temporal increase of huanglongbing in citrus plots in south Florida. MCMC posterior density likelihood estimations are for local and background influences on disease spread between two assessment dates for selected individual plots. Contour maps represent the posterior density estimations *L*(*a*) between two assessment dates for each plot with a minimum of 2.5% increase in disease incidence between individual assessments. Plots in this figure demonstrate a predominance of background or primary spread of disease that originates from outside the plot areas.

In this smaller group of analyses, the largest probability category values (darkest contour color) of the posterior density *L(a)*, extends exclusively from the vertical ***b*** axis. The highest probability category for ***b*** (the background parameter associated with primary spread) varied from about 0.5 to 1.2 whereas the corresponding values of $\boldsymbol{a_2}$ (the local parameter relating to secondary spread) were of about 1.75 to 3.5 along the upper end of the parameter range of the $\boldsymbol{a_2}$ axis. These analyses indicated background or primary spread of disease that originated from outside the plot areas. This is the most dangerous kind of spread in that it indicates a spatial process of long distance or regional spread by infected psyllids. Primary spread from outside the plot is the most devastating because no amount of localspraying will stop psyllids from feeding on distant HLB-positive sources, migrating to uninfected trees at some distance, and transmitting the bacterial pathogen before succumbing to insecticides applied to the new trees they settle on. These results are consistent with the Ripley's *K* regional analyses indicating a long distance component to vector transmissions.

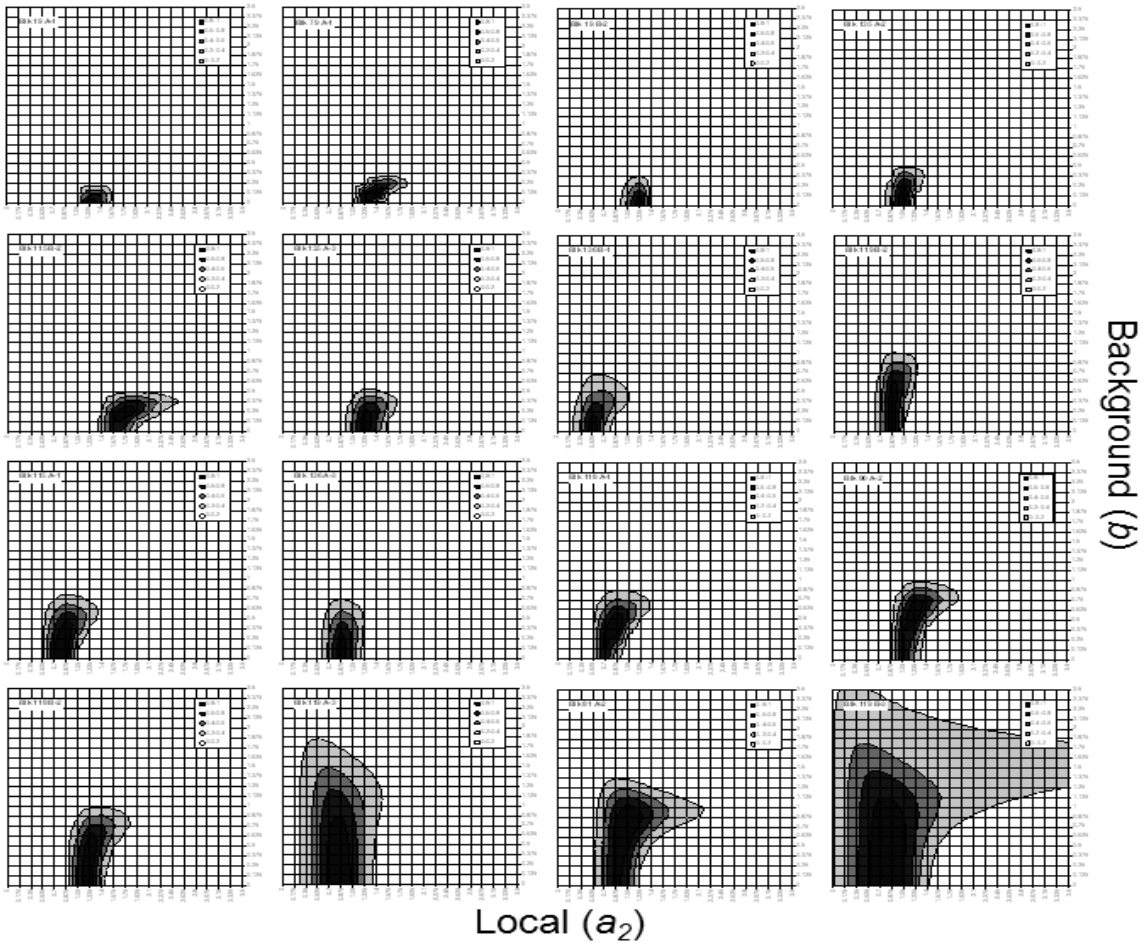

Fig. 4. Posterior density estimates of Markov-Chain Monte Carlo Simulation of the Spatio-temporal increase of huanglongbing in citrus plots in south Florida. MCMC posterior density likelihood estimations are for local and background influences on disease spread between two assessment dates for selected individual plots. Contour maps represent the posterior density estimations *L*(*a*) between two assessment dates for each plot with a minimum of 2.5% increase in disease incidence between individual assessments. Plots in this figure demonstrate posterior density estimates that provide evidence of secondary spread via predominantly midrange local interactions (that are not to nearest neighboring trees, but rather to trees that are nearby within a local area of influence) for dispersal of inoculum within the boundaries of the plots through time. The graph is arranged along rows and from top to bottom of the graphic with increasing posterior probability areas. See text for interpretation and details.

The contour graphs in Fig. 4 all show the largest probability category values of the posterior density L(*a*), corresponded to values of $\boldsymbol{a_2}$ (the local parameter relating to secondary spread) of about 0.7 to 1.3 along the lower end of the parameter range, joined the $\boldsymbol{a_2}$ axis, and the highest probability category for ***b*** (primary spread) varied from about 0.05 to 1.1. From these analyses, posterior density estimates provided evidence of secondary spread via predominantly midrange local interactions for inoculum dispersal within the boundaries of the plots through time. This spatial process is characterized by vector transmissions that are not to nearest neighboring trees, but rather to trees that are nearby within a local area of influence. The

prevalence of these two spatial processes is weighted much more heavily toward the secondary spatial process with only occasional evidence of background spread from external sources, i.e., random long distance transmissions of inoculum. Note that the graph is arranged along rows and from top to bottom of the graphic with increasing posterior probabilty contour areas. Those at the top of the graph indicate little to no evidence of background spread, whereas further down to the right of the individual graphs in Fig. 4, there are increasing indications of some level of background or primary spread. The final graph to the lower right indicates a lower probability contour actually descending to the ***b*** axis indicating a definite but subordinate influence of background spread.

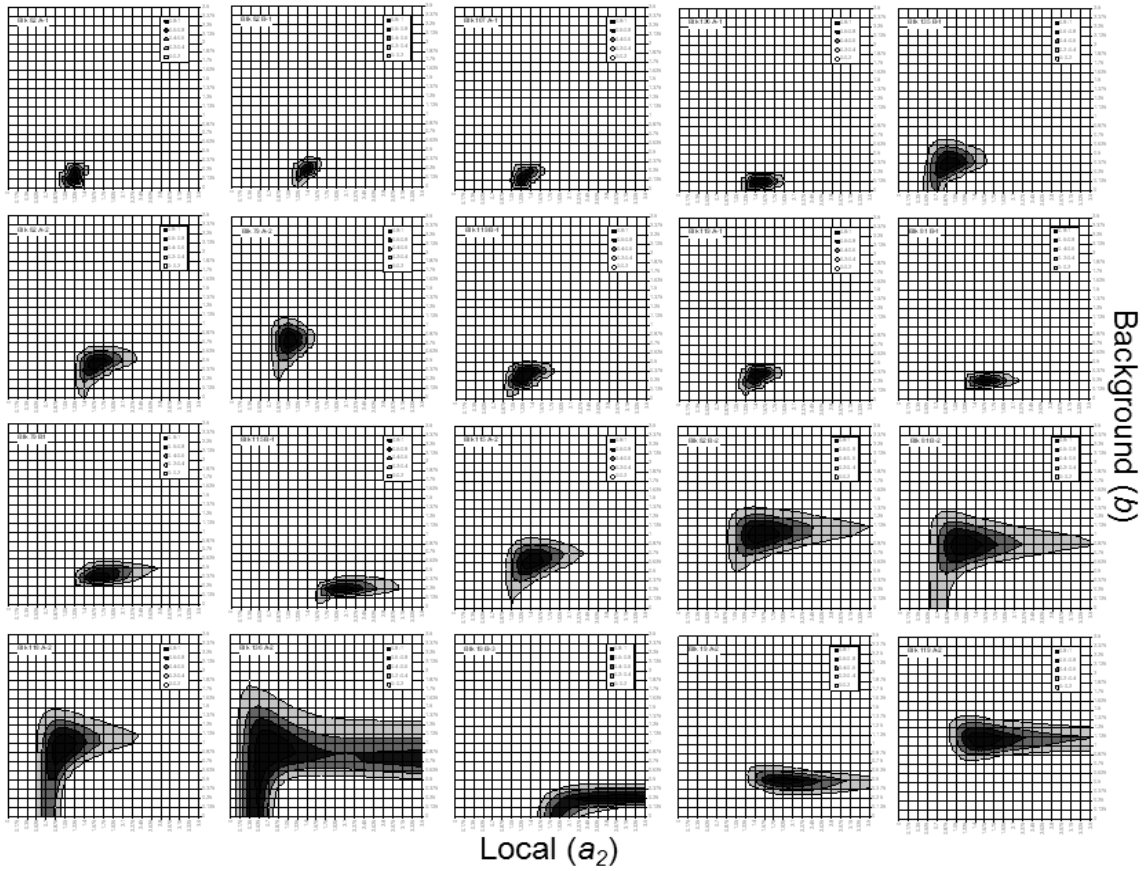

Fig. 5. Posterior density estimates of Markov-Chain Monte Carlo Simulation of the Spatio-temporal increase of huanglongbing in citrus plots in south Florida. MCMC posterior density likelihood estimations are for local and background influences on disease spread between two assessment dates for selected individual plots. Contour maps represent the posterior density estimations *L*(*a*) between two assessment dates for each plot with a minimum of 2.5% increase in disease incidence between individual assessments. Contour plots in this figure are the most common type and generally indicate that HLB spread occurs as an incessant mixture of two spatial processes, i.e., a continuous introduction of inoculum from outside the plot combined with local spread from within the plot occurring simultaneously.

Finally, a third category of posterior density contour graphs is shown in Fig. 5. These were perhaps the most common type of model result. In this case, the posterior density contours generally did not intersect either axis and indicated mixed spatial processes of primary and secondary spread occurring simultaneously. The top row

indicates posterior density contours confined near the a_2 axis but still with the highest contour levels not extended to that axis indicating a prevalence of secondary spread but with significant influence of simultaneous background spread as well. For the second row of graphs and the left portion of the third row, the contours rise above the a_2 axis and begin to increase in overall parameter space area, i.e., contours. This indicates a stronger but well mixed influence of both primary and secondary spread without a clear prevalence of either; however, the highest contour level is near the center of the a_2 range, indicating secondary spread that is mid range and neither nearest-neighbor nor short-range and local but somewhere in between. Lastly for the right two graphs on the third row, and all of the graphs on the fourth row, the lower probability density level contours begin to extend towards and generally intersect one or both axes, indicating a strong but mixed interaction of primary and secondary spread. The stochastic modeling analytical results characterized in Fig. 5 were the most common type and indicated generally that HLB spread occurred as an incessant mixture of these two processes interpreted as a continuous introduction of inoculum from outside the plot and simultaneous local spread from within the plot. Referring back to the Ripley's *K* analyses, the departure from CSR over the range of 0 to 3.5 km, confirms this mixture of primary spread (long distance to regional) and secondary (nearest neighbor to local) spread of HLB.

The data from this large commercial citrus plantation in south Florida are unique in several ways. Thry represent the earliest and most heavily HLB-infected commercial area in Florida. The data provide the first regional examination of the spatial distribution and spread of HLB. Even though the commercial industry in the area quickly instituted and/or increased psyllid control and initiated continuous orchard inspections and roguing of HLB-symptomatic trees, the age of the trees combined with the temporal latency of the disease provided a historical record of infection and spread that no amount of insect control or tree removal could mask within the two year period of data collection. Finally, the level of psyllid population/infestation in this planting was unprecedented compared to other recorded psyllid infestations, probably because the insect was relatively newly introduced to Florida and this area in particular and out of balance with environmental constraints. Thus this HLB epidemic is one of the worst recorded. That said, it demonstrates the rapid and destructive nature of the HLB-pathosystem during a time period when virtually no mitigating measures were yet influencing the epidemic and serves as seminal admonition to commercial citrus industries that would disregard and diminish the seriousness of HLB. The combined demonstrative evidence provided for regional spread and infection originating from outside plantings from this study, further substantiates the need to attempt control HLB regionally, and why control efforts on a local scale have always failed.

LITERATURE CITED

1. Aubert, B.
   1987. *Trioza erytreae* Del Guercio and *Diaphorina citri* Kuwayama (Homoptera: Psylloidae), the two vectors of citrus greening disease: Biological aspects and possible control strategies. Fruits 42: 149-162.
2. Aubert, B., M. Garnier, D. Guillaumin, B. Herbagyandono, L. Setiobudi, and F. Nurhadi
   1985. Greening, a serious threat for the citrus production of the Indonesian archipelago. Future prospects of integrated control. Fruits 40: 549-563.
3. Aubert, B., A. Sabine, P. Geslin, and L. Picardi
   1984. Epidemiology of the greening disease in Reunion Island before and after the biological control of the African and Asian citrus psyllas. Proc. Int. Soc. Citricult. 1: 440-442.
4. Bassanezi, R. B., L. A. Busato., A. Bergamin-Filho, L. Amorim, and T. R. Gottwald
   2005. Preliminary spatial analysis of huanglongbing in São Paulo, Brazil. In: *Proc. 16th Conf. IOCV*, 341:355. IOCV, Riverside, CA.
5. Castle, W. S., and T. R. Gottwald
   2005. Spatio-temporal analysis of tree decline losses among Navel orange trees on Swingle citrumelo rootstocks in two central Florida citrus groves. In: *Proc. 16th Conf. IOCV*, 370-380. IOCV Riverside, CA.
6. Catling, H. D. and P. R. Atkinson
   1974. Spread of greening by *Trioza erytreae* (Del Guercio) in Swaziland. In: *Proc. 6th Conf. IOCV*, 33-39. IOCV Riverside, CA.
7. Conover, W.J.
   1980. *Practical nonparametric statistics.*: John Wiley & Sons, New York. 496 pp.
8. Dingle, P. J.
   2003. *Statistical analysis of spatial point patterns*. 2nd ed. Oxford University Press 159 p.
9. Gatineau, F., H. T. Loc, N. D. Tuyen, T. M. Tuan, N. T. D. Hien, and N. T. N. Truc
   2006. Effects of two insecticide practices on population dynamics of *Diaphorina citri* and huanglongbing incidence in south Vietnam. Proc. Huanglongbing–Greening Int. Workshop, Ribeirão Preto, Brazil: 110.
10. Garnier, M., J. Latsille, and J. M. Bové
    1984. The greening organism is a Gram negative bacterium. In: *Proc. 9th Conf. IOCV*, 115-124. IOCV Riverside, CA.
11. Gibson, G. J.
    1997a. Investigating mechanisms of spatiotemporal epidemic spread using stochastic models. Phytopathology 87: 139-146.
12. Gibson, G. J.
    1997b. Markov chain Monte Carlo methods for fitting spatiotemporal epidemic stochastic models in plant pathology. Appl. Stat. 46: 215-233.
13. Gibson, G. J.
    1997c. Fitting and testing spatiotemporal stochastic models with applications in plant pathology. Plant Pathol. 45: 172-184.
14. Gottwald, T. R. and B. Aubert
    1988. Modeling of natural transmission of greening by vectors. Proc. 1st FAO/UNDP Citrus Greening Workshop, 16-23.
15. Gottwald, T. R., B. Aubert, and H. K. Long
    1990a. Spatial pattern analysis of citrus greening in Shantou, China. In: *Proc. 11th Conf. IOCV*, 421-427. IOCV Riverside, CA.
16. Gottwald, T. R., B. Aubert, and X. Z. Zhao
    1989. Preliminary analysis of citrus greening (Huanglungbin) of China and French Reunion Island. Phytopathology 79: 687-693.
17. Gottwald, T. R., J. V. da Graça, and R. B. Bassanezi
    2007. Citrus Huanglongbing: The pathogen, its epidemiology, and impact. Plant Health Progr. doi:10.1094/PHP-2007-0906-01-RV.
18. Gottwald, T. R., G. Gibson, S. M. Garnsey, and M. Irey
    1999. Examination of the effect of aphid vector population composition on the spatial dynamics of citrus tristeza virus spread via stochastic modeling. Phytopathology 89: 603-608.

19. Gottwald, T. R., C. I. Gonzales, and B. G. Mercado
1990b. Analysis of the distribution of citrus greening in groves in the Philippines. In: *Proc. 11th Conf. IOCV*, 414-420. IOCV, Riverside, CA.
20. Gottwald, T. R., S. R. Palle, H. Miao, M. Seyran, M. Skaria, and J. V. da Graça
2005. Assessment of the possibility of natural spread of citrus psorosis disease. In: *Proc. 16th Conf. IOCV*, 240-250. IOCV, Riverside, CA.
21. Illian, J., A. Penttinen, H. Stoyan, and D. Stoyan
2008. *Statistical analysis and modelling of spatial point patterns.* John Wiley and Sons, Ltd. 534 p.
22. Martinez, A. L. and J. M. Wallace
1967. Citrus leaf mottle-yellows disease in the Philippines and transmission of the causal virus by a psyllid, *Diaphorina citri*. Plant Dis. Rep. 51: 692-695.
23. McLean, A. P. D. and P. C. J. Oberholzer
1965. Citrus psylla, a vector of the greening disease of sweet orange. S. Afr. J. Agr. Sci. 8: 297-298.
24. Ward, J. S., and F. J. Ferrandino
1999. New derivation reduces bias and increases power of Ripley's L index. Ecol. Modeling 116: 225-36.
25. Zhao, X. Y.
1981. Citrus yellow shoot (Huanglungbin) in China: a review. Proc. Int. Soc. Citriculture 466-469.